

# Stabilizer Code-Generic Universal Fault-Tolerant Quantum Computation

Nicholas J.C. Papadopoulos<sup>1,\*</sup> and Ramin Ayanzadeh<sup>1</sup>

<sup>1</sup>University of Colorado Boulder, Department of Computer Science,  
Boulder, CO, 80309, USA

\*Corresponding author. Email: nicholas.papadopoulos@colorado.edu

## Abstract

Fault-tolerant quantum computation allows quantum computations to be carried out while resisting unwanted noise. Several error correcting codes have been developed to achieve this task, but none alone are capable of universal quantum computation. This universality is highly desired and often achieved using additional techniques such as code concatenation, code switching, or magic state distillation, which can be costly and only work for specific codes. This work implements logical Clifford and T gates through novel ancilla-mediated protocols to construct a universal fault-tolerant quantum gate set. Unlike traditional techniques, our implementation is deterministic, does not consume ancilla registers, does not modify the underlying data codes or registers, and is generic over all stabilizer codes. Thus, any single code becomes capable of universal quantum computation by leveraging helper codes in ancilla registers and mid-circuit measurements. Furthermore, since these logical gates are stabilizer code-generic, these implementations enable communication between heterogeneous stabilizer codes. These features collectively open the door to countless possibilities for existing and undiscovered codes as well as their scalable, heterogeneous coexistence.

## 1 Introduction

Quantum computing promises exponential speedups for certain classes of problems, but its practical realization remains unreliable due to the fragile nature of quantum information. Quantum bits (qubits) are susceptible to decoherence and operational noise, necessitating error-resistant protocols.

Quantum error correction (QEC) uses redundant information to protect against such error-causing noise by encoding the information of a quantum state using a collection of qubits, called a logical qubit. Fault-tolerant protocols use these encodings to perform error-resistant quantum computations. A central challenge in fault-tolerant quantum computing is efficiently implementing a set of gates that can perform any quantum computation, called a universal gate set.

All QEC codes support only a limited set of transversal logical gates, which are logical gates (gates that act on logical qubits) that can be performed bit-wise with physical gates and are inherently fault-tolerant. Hence, additional techniques must be used to fault-tolerantly perform any non-native logical gates. Established techniques often include code concatenation [1], code switching [2], or magic state distillation [3]. However, these techniques are often special procedures only available on the codes for which they were designed, or they are expensive and complicated.

Code concatenation is limited by the distance of their particular codes, and generalizing these codes to arbitrary distances can be costly if not impossible. Code switching [2, 4–7], often having the same limitations as code concatenation, transfers information between differently encoded registers. Magic state distillation [3, 8, 9] prepares many noisy copies of special quantum states that can then be used to output fewer copies of the quantum state with higher fidelity. These purified quantum states can then implement non-Clifford gates via gate teleportation [10]. This process is generally considered costly; Stein et al. describe it as having “expensive, if not prohibitive cost when scaling” [7]. Magic state distillation is nondeterministic and consumes ancilla resources, making the process unpredictable and costly.

We propose a novel, stabilizer code-generic framework for universal fault-tolerant quantum computation that relies on additional ancilla qubits for only mediation. We label techniques as ancilla-mediated if they use ancilla registers only as a means of communication or gate transformation without storing data themselves. Although no single code can have a transversal implementation of a universal gate set [11], our novel technique of ancilla-mediation combined with helper codes achieves universality without relying on previously established techniques. In contrast with code concatenation and code switching, we achieve universal fault-tolerant quantum computation on arbitrary, heterogeneous stabilizer codes (i.e., stabilizer code-generic). The data information always remains in its initial codes and registers, thereby preserving the properties of the underlying codes, including their distances and error correcting capabilities. In contrast with magic state distillation, our technique is deterministic and does not consume ancilla reg-

isters, making the additional registers reusable.

We target the Clifford+ $T$  logical gate set, which is a known universal gate set [12–14], while also supporting operation between data encoded in different QEC codes. Both of these tasks are achieved through the use of ancilla registers encoded with the generalized Shor code ( $GSC$ ) [15]. The particularly useful properties of this code enable transversal logical controlled-X and controlled-Z gates targeting any stabilizer code. In addition to  $GSC$ , one additional stabilizer code that has a fault-tolerant implementation of a  $T$  logical gate must be used to achieve the full, universal set. For example, triorthogonal codes are a well-documented class of such codes [16, 17].

Throughout the paper, we will use the term controlled-flip to encompass controlled-X and controlled-Z logical gates. We use the term stabilizer-generic gate (e.g., stabilizer-generic Hadamard gate) to denote a logical gate that can be performed on any arbitrary stabilizer code or codes.

First, we explain how to use the Hadamard basis of  $GSC$ , to which we refer as  $GSCH$ , to fault-tolerantly perform controlled-flip logical gates, where the register encoded with  $GSCH$  is the control, targeting any data encoding. This inherently extends to allow  $GSC$  to perform these logical gates when they are surrounded by Hadamard logical gates, as the Hadamards simply act to change the basis of the encoding. This further extends to allow a stabilizer-generic Hadamard gate on any data encoding, as the logical Hadamard gate can be composed of only logical controlled-flip gates controlled by an ancilla register. We then describe how to construct a stabilizer-generic controlled-flip gate between any two data encodings using the same techniques as are used in the stabilizer-generic Hadamard gate. Finally, we show that a stabilizer-generic rotation about the Z-axis, which includes a stabilizer-generic  $T$  gate, can be performed by entangling the data encoding, using the stabilizer-generic controlled-X, with a code that can perform the desired Z-rotation fault-tolerantly. Constructing these logical gates, therefore, satisfies the Clifford+ $T$  universal gate set. In each of the stabilizer-generic gates, we first describe a fault-intolerant version as a blueprint for the gates we want to achieve, then we use ancilla-mediation with  $GSC$  to perform the blueprint fault-tolerantly.

Our method offers a scalable path toward architecture-independent quantum computing. By decoupling logical gates from code-specific constraints, this framework, using exclusively ancilla-mediated protocols, (1) enables universal fault-tolerant quantum computing for any stabilizer code and (2) supports diverse quantum QEC codes in heterogeneous systems, where distinct encodings can communicate without requiring knowledge of or adaptation to the others. These contributions can replace current, resource-intensive

Table 1: Notation used throughout the paper.

Notation	Meaning
$C_i$	An arbitrary stabilizer code
$ \psi\rangle_{C_i}$	$\alpha 0\rangle_{C_i} + \beta 1\rangle_{C_i}$
$O$	An arbitrary gate
$\bar{O}_{C_i}$	Logical gate $O$ acting on $C_i$
$\bar{O}_{C_i, C_j}$	Logical gate $O$ acting on $C_j$ and controlled by $C_i$

techniques such as magic state distillation and open the door for future research to use a myriad of both existing or yet undiscovered QEC codes, as well as their combinations, without the need to find specific universal gate implementations for each of them.

## 2 Results

### 2.1 Notation

Table 1 summarizes the following notation used throughout this work. We denote the stabilizer code protecting the  $i$ th logical qubit as  $C_i$ . This notation allows for heterogeneity;  $C_1$  and  $C_2$  may represent entirely different codes or architectures. For instance,  $C_1$  could be a Surface code while  $C_2$  is a Steane code, or  $C_1$  and  $C_2$  could be the first and second qubit, respectively, of a four-qubit code ( $[[4, 2, 2]]$ ) [18].

Let  $\mathbb{Z}$  denote the set of integers,  $\mathbb{Z}^+$  denote the set of positive integers,  $2\mathbb{Z} + 1$  denote the set of odd integers, and  $\mathbb{C}$  denote the set of complex numbers. Also let  $|\psi\rangle_{C_i} = \alpha|0\rangle_{C_i} + \beta|1\rangle_{C_i}$ , for some  $\alpha, \beta \in \mathbb{C}$  and  $|\alpha|^2 + |\beta|^2 = 1$ , be the state of some encoded logical qubit. Similarly, let  $|\phi\rangle_{C_i} = \alpha'|0\rangle_{C_i} + \beta'|1\rangle_{C_i}$  be the state of some different logical qubit. The subscript of a ket denotes the code with which the qubit is encoded, which may be  $C_i$  for some arbitrary code, or it may be specified with the abbreviation of a particular code.

Let  $O$  denote an arbitrary, single-qubit gate so that  $\bar{O}_{C_i}$  denotes its respective logical gate acting on code  $C_i$ .  $\bar{O}_{C_1, C_2}$  represents a logical controlled gate, controlled by  $C_1$ , targeting  $C_2$ .

## 2.2 The Generalized Shor Code and its Hadamard Basis

### 2.2.1 GSC

*GSC* generalizes the Shor code to have any number of “cat” states  $\frac{1}{\sqrt{2}}(|0\dots0\rangle + |1\dots1\rangle)$  (named after Schrödinger’s cat) along with any number of qubits per cat state. Let *GSC* take two parameters: the number of cat states,  $a$ , and the number of qubits per cat state,  $b$ . We mark these in subscripts when referring to a specific *GSC*,  $GSC_{a,b}$ . Each of these cat states are called a subregister of the code, and  $si$  denotes the  $i$ th subregister. Cat states are well-known and can be encoded using any number of cat state initialization techniques [19]. The logical computational basis states  $|x\rangle_{GSC_{a,b}}$ , for  $x \in \{0, 1\}$  specifying the logical state  $|x\rangle$  encoded with  $GSC_{a,b}$ , are therefore

$$|x\rangle_{GSC_{a,b}} = \frac{1}{\sqrt{2^a}} \left( |0\rangle^{\otimes b} + (-1)^x |1\rangle^{\otimes b} \right)^{\otimes a}. \quad (1)$$

For example, the original Shor code is a  $GSC_{3,3}$  code with computational basis states

$$\begin{aligned} |0\rangle_{GSC_{3,3}} &= \frac{(|000\rangle + |111\rangle)(|000\rangle + |111\rangle)(|000\rangle + |111\rangle)}{2\sqrt{2}} \\ |1\rangle_{GSC_{3,3}} &= \frac{(|000\rangle - |111\rangle)(|000\rangle - |111\rangle)(|000\rangle - |111\rangle)}{2\sqrt{2}}. \end{aligned} \quad (2)$$

*GSC* has Z-stabilizers consisting of Z gates on pairs of adjacent qubits in each subregister, formally given by Eq. (3) with  $0 \leq i < a(b-1)$ ,

$$g_z(i, b) = Z_{q(i,b)} Z_{q(i,b)+1} \quad (3)$$

where  $q(i, b) = \lfloor i/(b-1) \rfloor b + i\%(b-1)$ . X-stabilizers consist of X gates on all qubits in pairs of adjacent subregisters, formally given by Eq. (4) with  $0 \leq i < a-1$ ,

$$g_x(i) = \prod_{j=bi}^{bi+2b-1} X_j. \quad (4)$$

In equations (3) and (4),  $Z_j$  and  $X_j$  are Z and X single-qubit gates acting on the  $j$ th qubit of the register. The operators for  $GSC_{a,b}$  are

$$\bar{Z} = \prod_{j=0}^{b-1} X_j, \quad \bar{X} = \prod_{j=0}^{a-1} Z_{aj}. \quad (5)$$

An example of these stabilizers can be found in Supplementary Note 4.3, and an image depicting  $GSC_{3,3}$  is shown in Fig. 1.

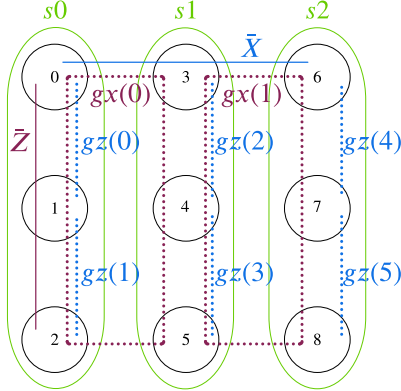


Figure 1:  $GSC_{3,3}$  in a grid structure. Data qubits are represented by black circles with center labels. The  $i$ th subregister,  $s_i$ , is labeled and circled in green. Red operators indicate a collection of X gates, while blue operators indicate a collection of Z gates. Hence, the qubits used for the  $\bar{X}$  logical gate are shown intersecting the horizontal, solid blue line, and those used for the  $\bar{Z}$  logical gate are shown intersecting the vertical, solid red line. Those used for the X-stabilizers are shown intersecting the dotted, red squares, and those used for the Z-stabilizers are shown intersecting the dotted, blue lines.

### 2.2.2 GSCH

$GSCH$  serves as  $GSC$ 's Hadamard dual, allowing measurements in the X-basis of either code without an explicit application of a physical Hadamard gate.  $GSCH$ , similarly to  $GSC$ , takes  $a$  and  $b$  as parameters and can be labeled  $GSCH_{a,b}$ . The logical computational basis states  $|x\rangle_{GSCH_{a,b}}$ , for  $x \in \{0, 1\}$ , are

$$|x\rangle_{GSCH_{a,b}} = \sum_{\substack{0 \leq i < 2^a \\ \text{wt}(i) \equiv x \pmod{2}}} \bigotimes_{j=0}^{a-1} |i_j\rangle^{\otimes b} \quad (6)$$

where  $\text{wt}(i)$  denotes the Hamming weight of  $i$ , i.e., the number of 1s in its binary representation, and  $i_j = \lfloor \frac{i}{2^j} \rfloor \pmod{2}$ , i.e., the  $j$ th bit of  $i$ . Essentially, the  $|0\rangle_{GSCH_{a,b}}$  consists of the basis states in  $|0\rangle_{GSC_{a,b}}$  that have an even number of subregisters in the  $|1\dots1\rangle$  state, and  $|1\rangle_{GSCH_{a,b}}$  consists of the remaining basis states in  $|0\rangle_{GSC_{a,b}}$ . An example of these states can be more explicitly seen in Supplementary Note 4.3. The generators are the same as

the corresponding  $GSC_{a,b}$ , but the logical operators are switched,

$$\bar{Z}_{GSCH_{a,b}} = \bar{X}_{GSC_{a,b}}, \quad \bar{X}_{GSCH_{a,b}} = \bar{Z}_{GSC_{a,b}}. \quad (7)$$

### 2.3 Controlled-flips Using the Generalized Shor Code

Throughout the rest of this paper, we imply the parameters  $a$  and  $b$  from context when  $GSC$  and  $GSCH$  appear without subscripts. Unless stated otherwise, let  $a \in 2\mathbb{Z} + 1$  such that  $a \geq 3$ , and let  $b \in \mathbb{Z}^+$  such that  $b \geq \max(|\bar{X}_{C1}|, |\bar{Z}_{C1}|)$  and  $b \geq 3$ . Here,  $|\bar{O}_{C1}|$  denotes the number of physical non-identity gates comprising  $\bar{O}_{C1}$ .

$GSCH$  has a useful capability, provided there are an odd number of cat states, to act as a control register targeting any data encoding when performing logical controlled-flip gates. Similar to Shor's measurement procedure, it uses its subregisters to perform the data encoding's transversal logical flip gate in a bit-wise fashion. Crucially, the structure of these codes allows transformations of  $GSC$  into  $GSCH$  without an explicit Hadamard gate by performing logical controlled-flip gates from the cat states to a data register, separating even and odd cat state parities by the flipped data register. Since these codes are error-correcting codes, they can resist errors throughout the procedure to allow for fault-tolerant computation.

#### 2.3.1 Flips Controlled By the GSCH

**Lemma 2.1** *Given the initial state  $|\psi\rangle_{GSCH} |\phi\rangle_{C1}$ , one can fault-tolerantly perform the logical gate  $\bar{O}_{GSCH,C1}$  for any flip gate  $O \in \{X, Z\}$ .*

In the same vein as Shor's measurement procedure, one can transversally perform  $\bar{O}_{si,C2}$  using each sequential subregister of  $GSCH$  with error correction between each logical gate. However, in order to perform the intermediate error corrections, the X-stabilizers of  $GSCH_{a,b}$  need to be temporarily modified after each  $i < a - 1$  since the code space is temporarily changed until all iterations are performed. The modified  $j$ th X-stabilizer after each  $i$  is (see Supplementary Note 1)

$$g'_x(i, j) = g_x(j) (\bar{O}_{C2})^{\delta_{ij}}, \quad (8)$$

where  $\delta_{ij} = \begin{cases} 1 & i = j \\ 0 & i \neq j \end{cases}$  is the Kronecker delta function. An example of these

modified stabilizers is shown in Fig. 2. After the last  $\bar{O}_{si,C2}$ , the stabilizers return to normal.

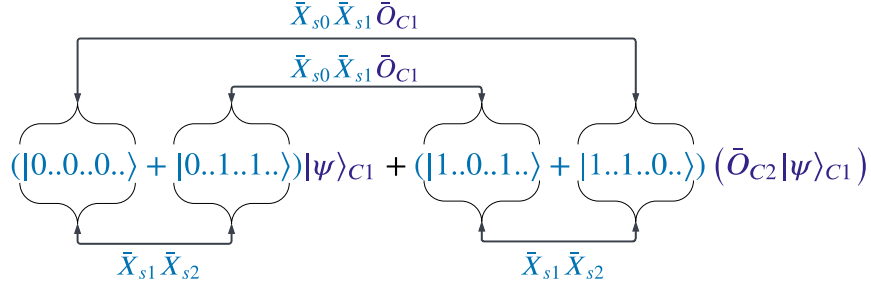


Figure 2: The transformation of states via the modified  $GSCH_{3,b}$  X-stabilizers for the first iteration of  $\bar{X}_{GSCH_{3,b},C1}$ , which performs  $\bar{X}_{s1,C1}$ , where the  $GSCH_{3,b}$  register encodes  $|0\rangle_{GSCH_{3,b}}$ . The arrows indicate which pairs of states are transformed into each other given a stabilizer.  $|a..b..c..\rangle$  is shorthand for  $\bigotimes_{i \in \{a,b,c\}} |i\rangle^{\otimes b}$ . Colors are used as a visual aid to distinguish different encodings.

After having the modified stabilizers, both the modified  $GSCH$  stabilizers and the data encoding stabilizers will be combined into one large code with two independently correctable partitions. So, using a  $GCSH_{3,3}$  code with data encoded with a distance 3 code, the combined code can correct up to one error in each partition. This allows for the correction of errors that have propagated from one partition to the other.

However, we can limit the number of combinations because the only additional errors we need to correct are when there is an error propagation either forward to the target qubit or back to the control qubit. For a forward propagation to occur in this scheme, (1) the errors on the  $GSCH$  partition include an  $X$  error on one of the qubits on which  $g_x(i)$  acts, and (2) the errors on the  $C1$  partition include an error on one of the qubits on which  $\bar{Z}_{C1}$  acts, and that error is either a  $Y$  error or commutes with the  $\bar{Z}_{C1}$  operator. For backwards propagation to occur, (1) the errors on the  $GSCH$  partition include a  $Z$  error on one of the qubits on which  $g_x(i)$  acts, and (2) the errors on the  $C1$  partition include an error that anticommutes with the  $\bar{Z}_{C1}$  operator. Therefore, we only need to account for additional syndromes if the error they detect has one of these two pairs of qualities. An example along with further elaboration on the modified stabilizers and additional correctable errors can be found in Supplementary Note 1.

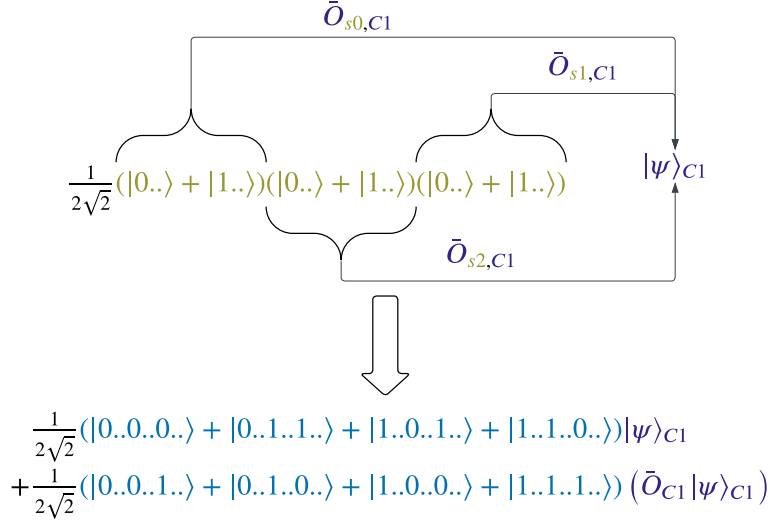


Figure 3: Diagram of the fault-tolerant process to perform logical flip gate  $\bar{O}_{GSC_{3,b},C1}$ .  $(|0..⟩ + |1..⟩)$  is shorthand for  $(|0\rangle^{\otimes b} + |1\rangle^{\otimes b})$ , and  $|a..b..c..\rangle$  is shorthand for  $\bigotimes_{i \in \{a,b,c\}} |i\rangle^{\otimes b}$ . Colors are used as a visual aid to distinguish different encodings.

### 2.3.2 Flips Controlled by GSC Between Hadamards

**Lemma 2.2** *Given the initial state  $|0\rangle_{GSC}|\psi\rangle_{C1}$ , one can fault-tolerantly perform the logical gates  $\bar{H}_{GSC}\bar{O}_{GSC,C1}\bar{H}_{GSC}$  for any flip gate  $O \in \{X, Z\}$ .*

Noting that we can change the helper encoding that a logical gate acts on by code surrounding the logical gate with logical Hadamards, one can see that

$$\begin{aligned}
& \bar{H}_{GSC}\bar{O}_{GSC,C1}\bar{H}_{GSC}(|0\rangle_{GSC}|\psi\rangle_{C1}) \\
& = \bar{H}_{GSC}\bar{H}_{GSC}^\dagger\bar{O}_{GSCH,C1}\bar{H}_{GSC}\bar{H}_{GSC}(|0\rangle_{GSC}|\psi\rangle_{C1}) \\
& = \bar{O}_{GSCH,C1}(|0\rangle_{GSC}|\psi\rangle_{C1}).
\end{aligned} \tag{9}$$

Thus, simply performing the operation in Lemma 2.1 will accomplish the desired state. An example of the effect of this procedure is shown in Fig. 3.

## 2.4 Stabilizer-Generic Gates

First, we present the fault-intolerant versions of stabilizer-generic Hadamard and controlled-flip gates as an overall plan to follow. When explaining these fault-intolerant protocols, we use a single-qubit ancilla register. This is only

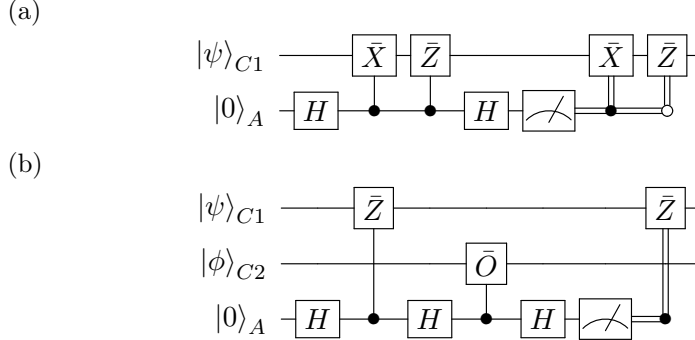


Figure 4: Circuit representation of fault-intolerant stabilizer-generic (a)  $\bar{H}_{C1}$  and (b)  $\bar{O}_{C1,C2}$  gates. The  $A$  subscript denotes a single-qubit ancilla register, and  $C1$  denotes an arbitrary target code.

a demonstrative helper, whose register will be labeled with the subscript  $A$  and whose role will be made fault-tolerant subsequently. Fig. 4a results in the desired Hadamard state  $(\alpha + \beta)|0\rangle_{C1} + (\alpha - \beta)|1\rangle_{C1}$ , while Fig. 4b results in the desired controlled-flip state  $\alpha|0\rangle_{C1}|\phi\rangle_{C2} + \beta|1\rangle_{C1}(\bar{O}_{C2}|\phi\rangle_{C2})$  (see Supplementary Note 4.1 and Supplementary Note 4.2 for the equation derivations).

Note that these are not limited to single-logical-qubit QEC codes. Consider, for example, a  $C1$  that refers to the second qubit of a code  $E$  encoding two logical qubits. Then,  $\bar{H}_{C1}$  applied to  $|\psi\rangle_E = \alpha|00\rangle_E + \beta|01\rangle_E + \gamma|10\rangle_E + \delta|11\rangle_E$  results in the state  $\alpha|0+\rangle_E + \beta|0-\rangle_E + \gamma|1+\rangle_E + \delta|1-\rangle_E$ .

Let the maximum number of physical gates between  $\bar{X}_{C1}$  and  $\bar{Z}_{C1}$  be  $|\mathcal{L}|$  for some  $C1$  on which an ancilla register will target. The following implementations use ancilla registers encoded with  $GSC_{a,b}$ , where  $b \geq |\mathcal{L}|$  and  $a$  is an odd integer.  $a$  and  $b$  must be at least 3 in order to correct at least one arbitrary error, but in general one would likely want  $a, b \geq d$ , where  $d$  is the distance of  $C1$ .

#### 2.4.1 Hadamard

**Theorem 2.3** *Given the initial state  $|0\rangle_{GSC}|\psi\rangle_{C1}$ , one can fault-tolerantly perform a stabilizer-generic Hadamard gate  $\bar{H}_{C1}$ .*

First, encode an ancilla register in  $|0\rangle_{GSC}$  that will target  $|\psi\rangle_{C1}$ . Ob-

serving that the following identities hold by Eq. (9),

$$\begin{aligned}
& \bar{H}_{GSC} \bar{Z}_{GSC,C1} \bar{X}_{GSC,C1} \bar{H}_{GSC} (|0\rangle_{GSC} |\psi\rangle_{C1}) \\
&= (\bar{H}_{GSC} \bar{Z}_{GSC,C1} \bar{H}_{GSC}) (\bar{H}_{GSC} \bar{X}_{GSC,C1} \bar{H}_{GSC}) (|0\rangle_{GSC} |\psi\rangle_{C1}) \quad (10) \\
&= \bar{Z}_{GSCH,C1} \bar{X}_{GSCH,C1} (|0\rangle_{GSC} |\psi\rangle_{C1}),
\end{aligned}$$

we can thus fault-tolerantly perform the first four gates in Fig. 4a by performing two gates of Lemma 2.2, as shown in Fig. 5a.

#### 2.4.2 Controlled-Flips

**Theorem 2.4** *Given the initial state  $|0\rangle_{GSC} |\psi\rangle_{C1} |\phi\rangle_{C2}$ , one can fault-tolerantly perform stabilizer-generic gate  $\bar{O}_{C1,C2}$  for any flip gate  $O \in \{X, Z\}$ .*

Using identities from Eq.(9), we can observe the following identities:

$$\begin{aligned}
& \bar{H}_{GSC} \bar{O}_{GSC,C2} \bar{H}_{GSC} \bar{Z}_{GSC,C1} \bar{H}_{GSC} (|0\rangle_{GSC} |\psi\rangle_{C1} |\phi\rangle_{C2}) \\
&= \bar{H}_{GSC} \bar{O}_{GSC,C2} \bar{Z}_{GSCH,C1} (|0\rangle_{GSC} |\psi\rangle_{C1} |\phi\rangle_{C2}) \quad (11) \\
&= \bar{H}_{GSC} \bar{H}_{GSC} \bar{O}_{GSCH,C2} \bar{H}_{GSC} \bar{Z}_{GSCH,C1} (|0\rangle_{GSC} |\psi\rangle_{C1} |\phi\rangle_{C2}) \\
&= \bar{O}_{GSCH,C2} \bar{H}_{GSC} \bar{Z}_{GSCH,C1} (|0\rangle_{GSC} |\psi\rangle_{C1} |\phi\rangle_{C2}).
\end{aligned}$$

Hence, after performing these logical gates, which we know how to do fault-tolerantly, we can measure  $\bar{Z}_{GSC}$  and apply the corrections described in Sec. 4b. The full fault-tolerant circuit is shown in Fig. 5b.

#### 2.4.3 Z-Rotations

**Theorem 2.5** *Given the initial state  $|0\rangle_{GSC} |\psi\rangle_{C1} |0\rangle_{RC}$ , where  $RC$  is a QEC code that has a fault-tolerant implementation of  $\bar{Z}^p = \begin{bmatrix} 1 & 0 \\ 0 & e^{i\pi p} \end{bmatrix}$ , one can fault-tolerantly perform stabilizer-generic gate  $(\bar{Z}^p)_{C1}$ .*

We now have all the tools necessary to finish our stabilizer-generic fault-tolerant universal gate set, which only needs an additional fault-tolerant implementation of Z-rotations. For this, we first encode an additional register in the logical zero state of some QEC code that has a fault-tolerant implementation of the desired rotation. For example, we can use the Steane code for a  $Z^{1/2} = S$  rotation or a  $[[15, 1, 3]]$  quantum Reed-Muller code for a  $Z^{1/4} = T$  rotation [4, 16, 20–22], which have transversal implementations of the desired rotations. Label this helper code, that has a fault-tolerant logical  $\bar{Z}^p$  gate, as  $RC$ .

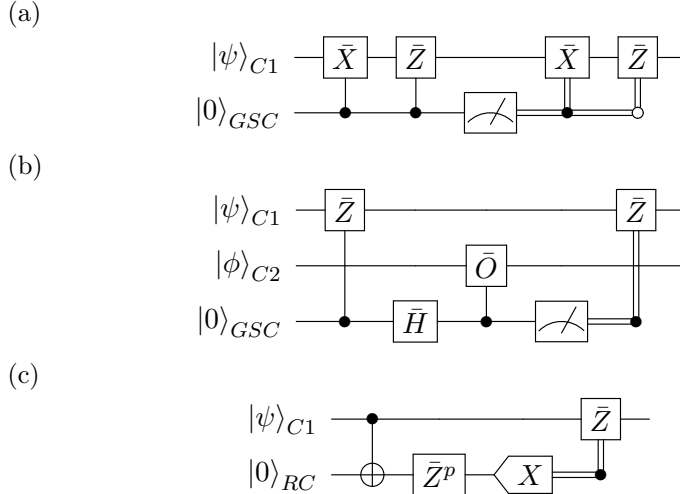


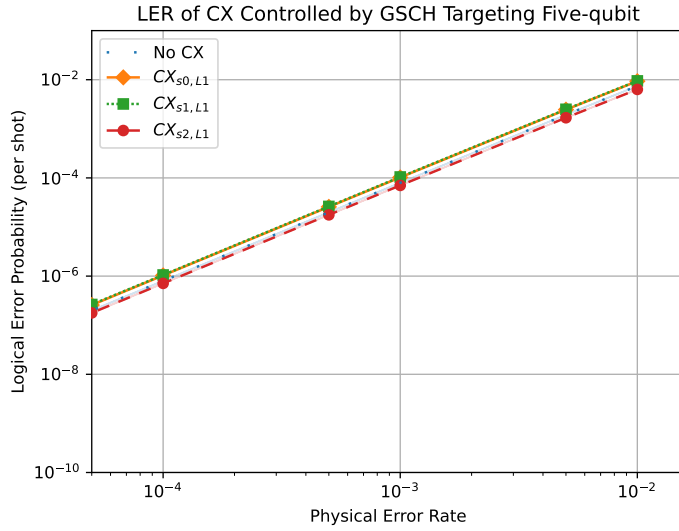
Figure 5: Circuit representation of fault-tolerant stabilizer-generic (a)  $\bar{H}_{C1}$ , (b)  $\bar{O}_{C1,C2}$ , and (c)  $\bar{T}_{C1}$  gates. Gates controlled by a  $GSC$  register use Lemma 2.2, and the double-qubit gate in (c) uses Theorem 2.4. The measurement in (c) is done in the  $X$ -basis. The  $RC$  subscript denotes a code that had a fault-tolerant implementation of a desired logical  $\bar{Z}^p$  gate.

By delegating all the work to previously built subroutines of logical Hadamard and controlled-NOT gates, one can perform a stabilizer-generic  $T$  gate via a  $T$  measurement [9], as shown in Fig. 5c.

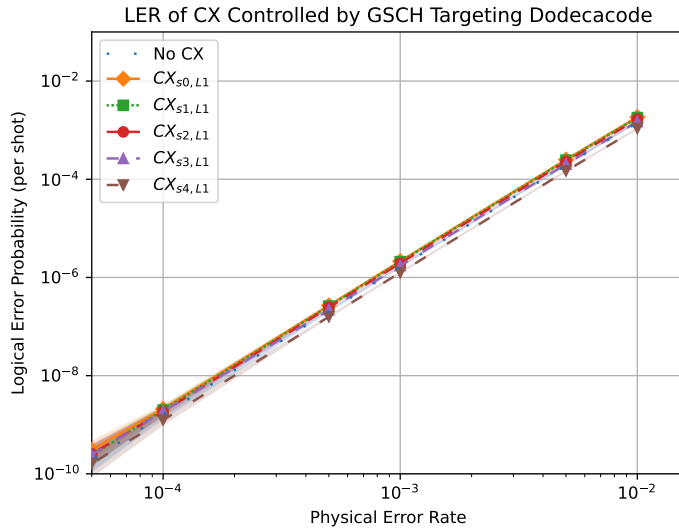
## 2.5 Validation

### 2.5.1 Logical Error Rate

The simulations described in Sec. 4 are shown in Fig. 6. This figure shows the logical error rate (LER) of each error correction step in the  $\bar{X}_{GSCH,C1}$  protocol scales on the same order as that of the individual codes acting independently. That is, for a target code  $C1$  and a  $GSC$  both of distance  $d$ , the LER of the combined code with modified stabilizers is  $O(p^{t+1})$ , where  $t = \lfloor \frac{d-1}{2} \rfloor$ , as expected. This confirms that each round of the protocol maintains the order of error-correcting capabilities of the constituent codes. Notably, after each subregister prior to the final one, the LER is observed to be slightly below the control case. This occurs because, at these intermediate stages, the stabilizer modifications momentarily combine  $GSC$  and  $C1$  into a single code with distance  $d$  (although often correcting up to  $2t$  errors).



(a)  $GSC_{3,5}$  as the control targeting  $C1$  as the five-qubit code.



(b)  $GSC_{5,5}$  as the control targeting  $C1$  as the dodecancode.

Figure 6: The LER of  $\bar{X}_{si,C1}$  for the  $i$ th subregister in  $GSC$ , showing each error correcting step of the protocol for  $\bar{X}_{GSCH,C1}$ . Shaded regions are default statistical fit uncertainties from the *stim* Python package.

The reduction comes because an error in the  $C1$  partition may propagate back into the  $GSC$  partition from the modified stabilizer, and vice versa. While often correctable, if the propagation leads to an uncorrectable number of errors in either of the partitions, the combined code cannot accurately correct it. After the final subregister, the codes return to being completely independent, thus matching the LER of the control case.

Upon close inspection, however, we do see a slight increase in performance after the final subregister. We attribute this to the fact that there is only one observable instead of the four that were measured during the control. Often times there may be an uncorrectable number of errors that cancel each other out from an even parity on the observable. If an uncorrectable number of errors occurred that cause a syndrome without an entry in the lookup table, the decoder predicts that no noise occurred. In such cases, which are more likely after the last subregister than during the control due to the larger observable, the decoder would predict an even parity with the observable, causing a false positive.

### 2.5.2 Stabilizer-Generic Gate Effects

With the preservation of LER demonstrated, we noiselessly simulated the full gate sequences described in Secs. 2.4.1, 2.4.2, and 2.4.3 to verify that they output the expected state vectors. These simulations acted on randomly generated states encoded with various QEC codes, and the resulting state vectors precisely matched the expected theoretical outcomes. These noiseless simulations support that the proposed protocols implement the correct logical transformations, thereby validating the fault-tolerant protocols for the stabilizer-generic gate set  $\{\bar{H}, \bar{CX}, \bar{T}\}$ .

For example, acting on the four-qubit code  $([[4, 2, 2]])$  [18], where the logical input state is  $|\psi\rangle_{C1} = \alpha|00\rangle_{C1} + \beta|01\rangle_{C1} + \gamma|10\rangle_{C1} + \delta|11\rangle_{C1}$  with randomly generated  $\alpha, \beta, \gamma$ , and  $\delta$ , the stabilizer-generic gates yielded the states given in Table 2. Further experiments included the implementation of the Deutsch-Jozsa algorithm [23] using  $GSC_{3,3}$  for two logical data qubits and one logical qubit for phase kickback. As expected, only the all-zero state was measured when the oracle was constant, and anything but the all-zero state was measured when the oracle was balanced.

## 3 Discussion

In this work, we have demonstrated a stabilizer-generic framework for universal fault-tolerant quantum computation. Our novel ancilla-mediated ap-

Table 2: Stabilizer-Generic gate effects on the  $[[4, 2, 2]]$  code.

Gate	Control Qubit / Target Qubit	Output
$\bar{H}$	N/A	$\frac{1}{\sqrt{2}}(\alpha + \beta) 00\rangle_{C1}$
		$+\frac{1}{\sqrt{2}}(\alpha - \beta) 01\rangle_{C1}$
	Second	$+\frac{1}{\sqrt{2}}(\gamma + \delta) 10\rangle_{C1}$
		$+\frac{1}{\sqrt{2}}(\gamma - \delta) 11\rangle_{C1}$
$\bar{X}_{C1, C2}$	First	$\alpha 00\rangle_{C1} + \beta 01\rangle_{C1}$
	Second	$+\delta 10\rangle_{C1} + \gamma 11\rangle_{C1}$
$\bar{T}$	N/A	$\alpha 00\rangle_{C1} + e^{i\pi/4}\beta 01\rangle_{C1}$
		$+\gamma 10\rangle_{C1} + e^{i\pi/4}\delta 11\rangle_{C1}$

proach effectively circumvents the Eastin-Knill theorem [11] without relying on constricting code-specific properties abundant in previous methods. Our results confirm that universal fault tolerance can be achieved for *any* stabilizer code provided that the appropriate Generalized Shor Code (GSC) and an appropriate code with a fault-tolerant logical  $\bar{T}$  gate can be prepared. Furthermore, the data remains encoded in the same physical space, so no modification to the data codes or partitions are required.

Crucially, this framework introduces capabilities previously inaccessible to fault-tolerant protocols. By decoupling the logical gate implementation from the underlying code structure, our method enables heterogeneous logical gates, such as a controlled-NOT operation between a surface code qubit and a Steane code qubit, without the need for complex code concatenation, code switching, or magic state distillation procedures. This renders any stabilizer code capable of interacting with any other stabilizer code, a previously unknown capability.

This framework thereby opens the door for a wide variety of future applications. For example, with the general convergence on distributed quantum computing [24], it may be beneficial to distribute computations across different types of hardware. Since certain hardware may be better suited for certain QEC codes, such as superconducting hardware for surface code or neutral atom hardware for quantum low-density parity-check codes codes,

heterogeneous communication between different stabilizer codes would facilitate distribution between different qubit modalities.

Notably, these stabilizer-generic gate protocols are not necessarily all required to construct a universal gate set for a particular code. These protocols serve as generic methods if specialized methods are unavailable. For example, the Surface Code already has a low-cost logical controlled-NOT gate using lattice surgery [13]. Hence, a computation using the Surface Code may opt to use lattice surgery for logical controlled-NOT gates, but still may find our stabilizer-generic  $T$  gate useful compared to magic state distillation. In other words, since each of our stabilizer code-generic gates do not rely on or change the underlying structure of any code, the computation is free to use them as-needed to optimize any part of the broader program. They serve as guaranteed methods to perform logical gates where specialized techniques are either not known or more costly.

Regarding the framework’s primary benefits, there is currently no alternative for generic cross-code entanglement, but magic state distillation is the standard alternative to making a single code universal. This strategy relies on distillation factories, which impose significant spacetime overheads and are by nature nondeterministic. That is, there is some probability of failure, and the process must be repeated indefinitely until a success occurs. In contrast, our protocol operates deterministically with a linear overhead of QEC rounds by code distance. As detailed in Supplementary Note 2, the qubit overhead for our protocol is dominated by the ancillary registers required for the Generalized Shor Code (GSC) states. While the physical scaling (qubits, gates) is polynomial, the overall cost is primarily spatial rather than temporal when compared to distillation-heavy protocols. A deeper analysis of tradeoffs between these two methods, investigating tradeoffs between runtime, number of qubits, and number of gates, is left for future work.

Ultimately, this framework paves the way for seamless communication within hybrid quantum architectures where, for example, high-threshold codes serve as robust memory and high-rate codes serve as efficient processing units. By providing a universal interface for heterogeneous codes, we move closer to a modular quantum computing stack and reduce the need to find univerality for any current or future stabilizer code. Overall, our approach provides a flexible and modular framework for universal fault-tolerant quantum computation, opening the doors for endless possibilities in the future of quantum computation.

## 4 Methodology

To validate the proposed fault-tolerant protocols, we conducted numerical simulation experiments divided into two main parts: (1) validation of the error correction during the execution of the logical  $CX$  gate controlled by  $GSCH$  (see Sec. 2.3.1) and (2) validation of the effects of the stabilizer-generic gates. Validation of the effects was conducted using the *cirq* Python package. This consisted of simulating the gate sequences and verifying the resulting state vector, as mentioned in Sec. 2.5.2.

Error correction was validated using the *stim* Python package [25]. The only additional QEC proposed in this paper is applied after each transversal logical controlled-flip gate controlled by a  $GSC$  or  $GCSH$  subregister. Hence, these simulations assume fault-tolerant encoding and measurement to isolate the capabilities of the modified stabilizers used in this process. This process is summarized as follows:

- **Control Case:** Both the  $GSC$  and the target code ( $C1$ ) were encoded ideally. Noise was applied to the data qubits as single-qubit depolarizing noise with probability  $p$ . Ideal error correction was performed with each code acting independently.
- **Test Case:** To test the error correction after a specific transversal operation,  $\bar{X}_{si,C1}$ , all preceding transversal gates  $\bar{X}_{sj,C1}$  with  $j < i$  were performed without noise. Single-qubit depolarizing noise was applied to every data qubit immediately before the final  $\bar{X}_{si,C1}$  gate.
- **Stabilizers and Decoding:** The stabilizers were based on those described in Sec. 2.3.1, which include the individual stabilizers for each code with one modified stabilizer, acting together as a single code. The decoders and a lookup-table were generated from this code’s symplectic matrix, mapping possible syndromes to the associated errors that would trigger them.

By scaling the  $GSC$  distance to match the distance of  $C1$ , we expect the order of the LER of each error correction round to closely match the control case. We therefore used the five-qubit code  $([[5, 1, 3]])$  [26] and the dodeca-code  $([[15, 1, 5]])$  [27] as two representative target QEC codes with distances  $d = 3$  and  $d = 5$ , respectively. Thus, the associated  $GSC$  registers used a distance-3  $GSC_{3,5}$  and a distance-5  $GSC_{5,5}$  code, respectively.

The measured observables were meant to divide all  $GSC$  data qubits and  $\bar{Z}_{C1}$  data qubits into the smallest portions that can be observed deterministically. These are split into two categories:

- **Untouched subregisters of  $GSC$ :** For the  $i$ th subregister  $si$ , one observable was defined for each subregister  $sj$  such that  $j > i$ . Their stabilizers consist of  $X$  gates on every qubit in the subregister  $sj$ , acting as a logical  $\bar{Z}$  measurement on the repetition code spanning  $sj$ . Since the  $\bar{X}_{si,C1}$  and prior  $\bar{X}$  gates do not affect these subregisters, this measurement yields an eigenvalue of  $+1$  under noiseless conditions.
- **Entangled subregisters:** For the  $i$ th subregister  $si$ , one observable was defined with a stabilizer consisting of  $Z$  gates on all qubits in subregisters  $sj$  where  $j \leq i$  as well as the qubits associated with  $\bar{Z}_{C1}$ . Since these subregisters are entangled with  $C1$ , their  $\bar{Z}$  values together with the  $C1$   $\bar{Z}$  value have even parity under noiseless conditions, yielding an eigenvalue of  $+1$ .

The total number of observables checked in each subregister experiment was  $a - i$ , where  $a$  is the total number of subregisters in  $GSC$ ,  $i$  is the index of the subregister being tested (starting at 0), and  $i = -1$  for the control case. One might wonder why these simulations measured all qubits in  $GSCH$  subregisters instead of just one, as the  $\bar{Z}_{GSCH}$  observable is described in the paper. This was done to keep the number of measured and observed data qubits consistent across tests on each  $si$ . These two observables, however, differ only by factors of elements of the stabilizers and hence have the same effect.

## Data Availability

All data generated or analyzed during this study are included in this published article (and its Supplementary Information files). The datasets used and/or analysed during the current study available from the corresponding author on reasonable request.

## Code Availability

The code used to simulate the protocols and generate the data in this study is available in the CU-Quantum/stabilizer-code-generic-ftqc repository at <https://doi.org/10.5281/zenodo.18248298>.

## References

- [1] Jochym-O'Connor, T. & Laflamme, R. Using concatenated quantum codes for universal fault-tolerant quantum gates. *Phys. Rev. Lett.* **112**, 010505 (2014). URL <https://link.aps.org/doi/10.1103/PhysRevLett.112.010505>.
- [2] Heußen, S. & Hilder, J. Efficient fault-tolerant code switching via one-way transversal cnot gates (2024). URL <https://arxiv.org/abs/2409.13465>. 2409.13465.
- [3] Knill, E. Fault-tolerant postselected quantum computation: Schemes (2004). URL <https://arxiv.org/abs/quant-ph/0402171>. quant-ph/0402171.
- [4] Anderson, J. T., Duclos-Cianci, G. & Poulin, D. Fault-tolerant conversion between the steane and reed-muller quantum codes. *Physical Review Letters* **113** (2014). URL <http://dx.doi.org/10.1103/PhysRevLett.113.080501>.
- [5] Butt, F., Heußen, S., Rispler, M. & Müller, M. Fault-tolerant code-switching protocols for near-term quantum processors. *PRX Quantum* **5**, 020345 (2024). URL <https://link.aps.org/doi/10.1103/PRXQuantum.5.020345>.
- [6] Li, C., Preskill, J. & Xu, Q. Transversal dimension jump for product qldpc codes (2025). URL <https://arxiv.org/abs/2510.07269>. 2510.07269.
- [7] Stein, S. *et al.* Architectures for heterogeneous quantum error correction codes (2024). URL <https://arxiv.org/abs/2411.03202>. 2411.03202.
- [8] Bravyi, S. & Kitaev, A. Universal quantum computation with ideal clifford gates and noisy ancillas. *Phys. Rev. A* **71**, 022316 (2005). URL <https://link.aps.org/doi/10.1103/PhysRevA.71.022316>.
- [9] Litinski, D. Magic state distillation: Not as costly as you think. *Quantum* **3**, 205 (2019). URL <http://dx.doi.org/10.22331/q-2019-12-02-205>.
- [10] Zhou, X., Leung, D. W. & Chuang, I. L. Methodology for quantum logic gate construction. *Phys. Rev. A* **62**, 052316 (2000). URL <https://link.aps.org/doi/10.1103/PhysRevA.62.052316>.

- [11] Eastin, B. & Knill, E. Restrictions on transversal encoded quantum gate sets. *Phys. Rev. Lett.* **102**, 110502 (2009). URL <https://link.aps.org/doi/10.1103/PhysRevLett.102.110502>.
- [12] Boykin, P. O., Mor, T., Pulver, M., Roychowdhury, V. & Vatan, F. On universal and fault-tolerant quantum computing: A novel basis and the quantum circuits for shor's algorithm. In *Proceedings of the 40th Annual Symposium on Foundations of Computer Science*, 486–494 (IEEE, 1999).
- [13] Horsman, D., Fowler, A. G., Devitt, S. & Meter, R. V. Surface code quantum computing by lattice surgery. *New Journal of Physics* **14**, 123011 (2012). URL <http://dx.doi.org/10.1088/1367-2630/14/12/123011>.
- [14] Jochym-O'Connor, T., Yu, Y., Helou, B. & Laflamme, R. The robustness of magic state distillation against errors in clifford gates (2012). URL <https://arxiv.org/abs/1205.6715>. 1205.6715.
- [15] Bacon, D. & Casaccino, A. Quantum error correcting subsystem codes from two classical linear codes. In *Proceedings of the 44th Annual Allerton Conference on Communication, Control, and Computing*, 529–534 (2006).
- [16] Bravyi, S. & Haah, J. Magic-state distillation with low overhead. *Physical Review A* **86** (2012). URL <http://dx.doi.org/10.1103/PhysRevA.86.052329>.
- [17] Haah, J. & Hastings, M. B. Codes and protocols for distilling t, controlled-s, and toffoli gates. *Quantum* **2**, 71 (2018). URL <http://dx.doi.org/10.22331/q-2018-06-07-71>.
- [18] Córcoles, A. D. *et al.* Demonstration of a quantum error detection code using a square lattice of four superconducting qubits. *Nature Communications* **6**, 7979 (2015). URL <https://www.nature.com/articles/ncomms7979>.
- [19] Prabhu, P. & Reichardt, B. W. Fault-tolerant syndrome extraction and cat state preparation with fewer qubits. *Quantum* **7**, 1154 (2023). URL <http://dx.doi.org/10.22331/q-2023-10-24-1154>.
- [20] Steane, A. M. Error correcting codes in quantum theory. *Phys. Rev. Lett.* **77**, 793–797 (1996). URL <https://link.aps.org/doi/10.1103/PhysRevLett.77.793>.

- [21] Knill, E., Laflamme, R. & Zurek, W. Threshold accuracy for quantum computation (1996). URL <https://arxiv.org/abs/quant-ph/9610011>. *quant-ph*/9610011.
- [22] Steane, A. Quantum reed-muller codes. *IEEE Transactions on Information Theory* **45**, 1701–1703 (1999).
- [23] Deutsch, D. & Jozsa, R. Rapid solution of problems by quantum computation. *Proc. R. Soc. Lond. A* **439**, 553–558 (1992). URL <https://doi.org/10.1098/rspa.1992.0167>.
- [24] Cuomo, D., Caleffi, M. & Cacciapuoti, A. S. Towards a distributed quantum computing ecosystem. *IET Quantum Communication* **1**, 3–8 (2020).
- [25] Gidney, C. Stim: a fast stabilizer circuit simulator. *Quantum* **5**, 497 (2021).
- [26] Laflamme, R., Miquel, C., Paz, J. P. & Zurek, W. H. Perfect quantum error correcting code. *Phys. Rev. Lett.* **77**, 198–201 (1996). URL <https://link.aps.org/doi/10.1103/PhysRevLett.77.198>.
- [27] Scott, A. J. Probabilities of failure for quantum error correction. *Quantum Information Processing* **4**, 399–431 (2005). URL <http://dx.doi.org/10.1007/s11128-005-0002-1>.
- [28] Tansuwanont, T., Pato, B. & Brown, K. R. Adaptive syndrome measurements for shor-style error correction. *Quantum* **7**, 1075 (2023). URL <http://dx.doi.org/10.22331/q-2023-08-08-1075>.

## Acknowledgements

This work utilized the Alpine high performance computing resource at the University of Colorado Boulder. Alpine is jointly funded by the University of Colorado Boulder, the University of Colorado Anschutz, Colorado State University, and the National Science Foundation (award 2201538).

Diagrams were created in Lucid (lucid.co).

## **Author contributions statement**

N.J.P. conceived the project, developed the protocols, and performed the experiments. R.A. supervised the work. Both authors wrote and reviewed the manuscript.

## **Competing Interests**

The authors declare no competing interests.

**Supplementary Information for:**  
 Stabilizer Code-Generic Universal Fault-Tolerant Quantum  
 Computation

**Supplementary Note 1 Flips Controlled by GSCH,  
 Modified Stabilizers**

Given  $|\phi\rangle_{GSCH_{a,b}} |\psi\rangle_{C1}$ , each subspace  $|0\rangle_{GSCH_{a,b}} |\psi\rangle_{C1}$  and  $|1\rangle_{GSCH_{a,b}} |\psi\rangle_{C1}$  will be further separated into two subspaces after each  $\bar{O}_{si,C1}$  for sequential  $si$  in  $GSCH_{a,b}$ . This section aims to show that

$$g'_x(i, j) = g_x(j) (\bar{O}_{C2})^{\delta_{ij}} \quad (S1)$$

serves as the modified  $j$ th X-stabilizer after performing  $\bar{O}_{si,C1}$ .

First recognize that, for any computational basis state  $|x\rangle_{GSCH_{a,b}}$ ,  $\bar{O}_{si,C1}$  splits the basis states of  $|x\rangle_{GSCH_{a,b}}$  by whether an even number of the first  $i$  cat states are 1s. An even number of these cancel the flip operation, while an odd number flips  $|\psi\rangle_{C1}$ . That is,

$$\begin{aligned} \left( \prod_{k=0}^i \bar{O}_{s(i-k),C1} \right) |x\rangle_{GSCH_{a,b}} |\psi\rangle_{C1} = \\ \sum_{\substack{0 \leq \ell < 2^a \\ \text{wt}(\ell) \equiv x \pmod{2}}} \bigotimes_{p=0}^{a-1} |\ell_p\rangle^{\otimes b} \left( (\bar{O}_{C1})^{\text{wts}(\ell,i)\%2} |\psi\rangle_{C1} \right), \end{aligned} \quad (S2)$$

where  $\text{wts}(\ell, i) = \sum_{q=0}^i (\lfloor \frac{\ell}{2^q} \rfloor \bmod 2)$  is the Hamming weight of the first  $i+1$  digits of the binary representation of  $\ell$ .

Hence, a stabilizer  $g_x(j)$ , since it acts on pairs of cat states, does not modify the parity of the subspaces unless only half of it acts on the subspace, which only happens when  $i = j$ . In that case, the codespace will be switched, and we must add  $\bar{O}_{C1}$  to the stabilizer in order to correctly swap an erroneous sign flip with the corresponding basis state of  $|x\rangle_{GSCH_{a,b}}$ .

Because the modified stabilizer now acts on both the  $GSCH_{a,b}$  and  $C1$  codes, the codes must be considered as one large code that can independently correct  $\lfloor \frac{d'-1}{2} \rfloor$  errors in the  $GSCH_{a,b}$  partition and  $\lfloor \frac{d-1}{2} \rfloor$  errors in

the  $C1$  partition, where  $d$  is the distance of  $C1$  and  $d' = \min(a, b)$  is the distance of  $GSC_{a,b}$ . However, we do not need to account for all possible combinations of errors on each partition. The only errors we need to correct, in addition to the correctable ones that occur in only one partition, are ones that anticommute with the  $\bar{Z}_{C1}$  logical gate and contain a  $Z$  error on one of the qubits in the  $GCSH$  partition on which the modified stabilizer acts.

Take, for example, a data encoding  $C1 = GSC_{3,3}$ . After performing the controlled flip logical gate controlled by the  $s0$  subregister of the helper, the symplectic representation of the large code is shown in Tab. S1. The additional errors to correct in this example, besides the errors that each partition could correct alone, are  $\{Z_k X_j : 0 \leq k < 6 \wedge j \in \{0, 3, 6\}\}$ . As a further example, the error  $Z_0, X_9$  would produce a syndrome where only  $g_6$  measures 1. This is because  $g_{12}$  will measure 0, as it anticommutes with both errors.

## Supplementary Note 2 Resource Overhead

Consider (1) a maximum number of qubits,  $n_{C1}$  in a target code with distance  $d_{C1}$ , (2) the number of qubits,  $n_{RC}$  in a code with distance  $d_{C1}$  that has a fault-tolerant implementation of a logical  $\bar{Z}^\theta$  gate, and (3)  $n_{MC} = \max(n_{C1}, n_{RC})$ . Then, a circuit using these codes to implement our stabilizer-generic Clifford+ $Z^\theta$  gate set incurs an overhead of up to

$$\begin{aligned} m &= O(d_{C1}) \\ N^{(2)} &= O((n_{MC})^4) \\ N^{(1)} &= O((d_{C1})^2 + n_{RC}) \\ n &= O((n_{MC})^2) \end{aligned} \tag{S3}$$

QEC rounds, double-qubit physical gates, single-qubit physical gates, and qubits, respectively.  $m$ , the additional number of QEC rounds, is due to the logical  $\bar{O}_{GSCH,C1}$  gate being performed in  $a$  sequential steps with QEC rounds performed after each one. Since there are a constant number of  $\bar{O}_{GSCH,C1}$  gates per stabilizer-generic gate, and  $a$  should generally be equal to  $d_{C1}$ ,  $m$  scales as  $O(d_{C1})$ . The results of the other metrics are explained in the following sections.

To determine the bounds for the Clifford+ $T$  gate set,  $RC = TC$ , one can use a triorthogonal code. Based on known constructions for triorthogonal codes [16], the number of qubits  $n_{TC}$  required for a target distance  $d_{TC} = d_{C1}$

Supplementary Table S1: The symplectic representation of the modified stabilizer,  $g_{12}$ , after performing  $\bar{X}_{s0,C1}$  during a  $\bar{X}_{GSCH_{3,3},C1}$  logical gate. Here,  $C1 = GSC_{3,3}$ .  $g_j$  represents the  $j$ -th generator. Qubit numbers are ordered 0-17 from left to right in each X and Z section.

	X									
	GSCH <sub>3,3</sub>					C1				
$g_0$	0	0	0	0	0	0	0	0	0	0
$g_1$	0	0	0	0	0	0	0	0	0	0
$g_2$	0	0	0	0	0	0	0	0	0	0
$g_3$	0	0	0	0	0	0	0	0	0	0
$g_4$	0	0	0	0	0	0	0	0	0	0
$g_5$	0	0	0	0	0	0	0	0	0	0
$g_6$	0	0	0	0	0	0	0	0	0	0
$g_7$	0	0	0	0	0	0	0	0	0	0
$g_8$	0	0	0	0	0	0	0	0	0	0
$g_9$	0	0	0	0	0	0	0	0	0	0
$g_{10}$	0	0	0	0	0	0	0	0	0	0
$g_{11}$	0	0	0	0	0	0	0	0	0	0
<b>g<sub>12</sub></b>	<b>1</b>	<b>1</b>	<b>1</b>	<b>1</b>	<b>1</b>	0	0	0	0	0
$g_{13}$	0	0	0	1	1	1	1	1	0	0
$g_{14}$	0	0	0	0	0	0	0	1	1	0
$g_{15}$	0	0	0	0	0	0	0	0	1	1
	Z									
	GSCH <sub>3,3</sub>					C1				
$g_0$	1	1	0	0	0	0	0	0	0	0
$g_1$	0	1	1	0	0	0	0	0	0	0
$g_2$	0	0	0	1	1	0	0	0	0	0
$g_3$	0	0	0	0	1	1	0	0	0	0
$g_4$	0	0	0	0	0	1	1	0	0	0
$g_5$	0	0	0	0	0	0	1	1	0	0
$g_6$	0	0	0	0	0	0	0	1	1	0
$g_7$	0	0	0	0	0	0	0	0	1	1
$g_8$	0	0	0	0	0	0	0	0	0	1
$g_9$	0	0	0	0	0	0	0	0	0	1
$g_{10}$	0	0	0	0	0	0	0	0	0	1
$g_{11}$	0	0	0	0	0	0	0	0	0	1
<b>g<sub>12</sub></b>	0	0	0	0	0	0	0	1	0	0
$g_{13}$	0	0	0	0	0	0	0	0	0	0
$g_{14}$	0	0	0	0	0	0	0	0	0	0
$g_{15}$	0	0	0	0	0	0	0	0	0	0

is bounded (see Supplementary Note 3) by

$$\begin{aligned} n_{TC} &= O\left((d_{TC})^2 \log^2 d_{TC}\right) \\ &= O\left((d_{C1})^2 \log^2 d_{C1}\right). \end{aligned} \quad (S4)$$

### Supplementary Note 2.1 Assumptions and Definitions

We define the following parameters, summarized in Table S2, for the ancilla and target codes. As in previous sections,  $GSC_{a,b}$  represents  $GSC$  with  $a$  cat states and  $b$  qubits per cat state.  $GSC_{a,b}$  therefore uses  $n_{GSC} = ab$  data qubits and  $s = ab - 1$  stabilizers. Its distance is  $d_{GSC} = \min(a, b)$ , allowing  $t_{GSC} = \lfloor(d_{GSC} - 1)/2\rfloor$  arbitrary errors to be corrected. It follows, then, that  $d_{GSC} \leq a, b$ .

$C1$ , here representing the largest target QEC code used in the system, has  $n_{C1}$  data qubits and distance  $d_{C1}$ .  $RC$ , representing a code having a transversal implementation of a desired  $\bar{Z}^p$  rotation, has  $n_{RC}$  data qubits. With no assumptions, the number of qubits per cat state  $b$  must be enough to perform a logical  $\bar{X}$  or  $\bar{Z}$  gate on either  $C1$  or  $RC$ . Thus,  $b \leq n_{MC}$ , where  $n_{MC} = \max(n_{C1}, n_{RC})$ . To match the code distance so that  $d_{GSC} = d_{RC} = d_{C1}$ , we set  $a = d_{RC} = d_{C1} \leq n_{C1}$ . Thus,  $a, b \leq n_{MC}$  and the correctable errors  $t_{GSC} = t_{RC} = t_{C1} < d_{C1}$ .

The overhead associated with initial encoding, logical state preparation, and non-stabilizer measurements are excluded, as these are implementation-specific. Error correction overhead for the target codes ( $C1, C2, \dots$ ) are also excluded, as these are considered part of the underlying system with or without stabilizer-generic gates. We assume a Shor-style stabilizer measurement procedure, requiring

- $r = d_{MC} \leq n_{MC}$  measurement rounds per QEC round [28].
- One double-qubit gate per gate in the stabilizer being measured.
- Up to  $t_{MC} = \lfloor(d_{MC} - 1)/2\rfloor$  single-qubit gates per QEC round.
- One ancilla qubit per gate in the stabilizer being measured.

### Supplementary Note 2.2 Double-Qubit Gate Overhead

Out of the  $s$  stabilizers of  $GSC$ ,  $z = a(b - 1)$  of them have 2 gates and  $x = a - 1$  of them have  $2b$  gates. Assuming the syndrome measurement

Supplementary Table S2: Resource Overhead Parameters and Bounds

Code	Data Qubits	Distance / Correctable Errors
$C1$	$n_{C1}$	$d_{C1} \leq n_{C1}$ $t_{C1} < d_{C1}$
$RC$	$n_{RC}$	$d_{RC} = d_{C1}$ $t_{RC} < d_{C1}$
$TC$	$n_{TC}$ $= O((d_{C1})^2 \log^2 d_{C1})$	$d_{TC} = d_{C1}$ $t_{TC} < d_{C1}$
$MC$	$n_{MC} = \max(n_{C1}, n_{RC})$	$d_{MC} = d_{C1}$ $t_{MC} < d_{C1}$
$GSC_{a,b}$	$n_{GSC} = ab$ $\leq (n_{MC})^2$	$d_{GSC} = d_{C1}$ $t_{GSC} < d_{C1}$

procedure requires a double-qubit controlled physical gate per stabilizer gate, the total number of double-qubit gates for syndrome extraction is

$$\begin{aligned}
 N_{GSC}^{(2)} &= r(2z + 2bx) \\
 &= r(2a(b-1) + 2b(a-1)) \\
 &= O(rab) \\
 &\leq O((n_{MC})^3).
 \end{aligned} \tag{S5}$$

Similarly, a QEC round for  $RC$  incurs an overhead of  $N_{RC}^{(2)} \leq (n_{RC})^3$  double-qubit physical gates because there are up to  $n_{RC}$  stabilizers, each with up to  $n_{RC}$  gates, and  $r \leq n_{RC}$  measurement rounds per QEC round.

Logical controlled-flips controlled by  $GSCH$  ( $\bar{O}_{GSCH,MC}$ ) are executed in  $a = d_{MC} \leq n_{MC}$  iterations. Each iteration performs up to  $b \leq n_{MC}$  double-qubit physical gates followed by error correction with a modified stabilizer. The modified stabilizer adds  $|\bar{O}_{MC}| \leq n_{MC}$  double-qubit physical gates to the unmodified syndrome extraction of  $N_{GSC}^{(2)}$ . Thus, the total double-qubit physical gate overhead for  $\bar{O}_{GSCH,C1}$  after  $a$  iterations is:

$$\begin{aligned}
 N_{\bar{O}_{GSCH,MC}}^{(2)} &= a \left( b + N_{GSC}^{(2)} + |\bar{O}_{MC}| \right) \\
 &\leq n_{MC} (n_{MC} + (n_{MC})^3 + n_{MC}) \\
 &= O((n_{MC})^4).
 \end{aligned} \tag{S6}$$

The stabilizer-generic Hadamard gate performs a logical  $\bar{X}_{GSCH,C1}$  gate followed by a logical  $\bar{Z}_{GSCH,C1}$  gate, resulting in  $N_{\bar{H}}^{(2)} = 2N_{\bar{O}_{GSCH,C1}}^{(2)} = O((n_{C1})^4)$  double-qubit physical gates. The stabilizer-generic controlled-flip gates perform a logical  $\bar{Z}_{GSCH,C1}$  gate, then a stabilizer-generic  $\bar{H}_{GSC}$  gate, then a logical  $\bar{O}_{GSCH,C1}$  gate. Combined,

$$\begin{aligned} N_{\bar{O}_{C1,C2}}^{(2)} &= N_{\bar{O}_{GSCH,C1}}^{(2)} + N_{\bar{H}}^{(2)} + N_{\bar{O}_{GSCH,C1}}^{(2)} \\ &= O((n_{C1})^4) \end{aligned} \quad (S7)$$

double-qubit physical gates are required.

The stabilizer-generic Z-rotation gate performs a stabilizer-generic  $\bar{O}_{C1,RC}$  gate, then a logical  $(\bar{Z}^p)_{RC}$  gate with error correction, then another stabilizer-generic  $\bar{O}_{C1,RC}$  gate. The logical  $(\bar{Z}^p)_{RC}$  gate only uses single-qubit physical gates and therefore does not contribute to the double-qubit physical gate overhead. However, the error correction after this gate is applied to the additional codes  $GSC$  and  $RC$ . Thus, the stabilizer-generic Z-rotation gate has a double-qubit physical gate overhead of

$$\begin{aligned} N_{\bar{Z}^p}^{(2)} &= N_{\bar{O}_{C1,RC}}^{(2)} + N_{GSC}^{(2)} + N_{RC}^{(2)} + N_{\bar{O}_{C1,RC}}^{(2)} \\ &= O((n_{MC})^4 + (n_{MC})^3 + (n_{RC})^3 + (n_{MC})^4) \\ &= O((n_{MC})^4). \end{aligned} \quad (S8)$$

The double-qubit physical gate overhead is summarized in Table S3.

### Supplementary Note 2.3 Single-Qubit Gate Overhead

Error recovery requires single-qubit physical gates (controlled by classical results), generally applying one single-qubit physical gate per error. Hence, error correction for  $GSC$  requires up to  $N_{GSC}^{(1)} = t_{GSC} < d_{C1}$  single-qubit physical gates. Similarly,  $RC$  requires  $N_{RC}^{(1)} = t_{RC} < d_{C1}$  single-qubit physical gates.

The rest of the single-qubit physical gate overhead follows the same logic as the double-qubit gate overhead, except  $(\bar{Z}^p)_{RC}$  additionally uses up to  $n_{RC}$  single-qubit physical gates for the the logical  $(\bar{Z}^p)_{RC}$  gate. The single-qubit physical gate overhead is summarized in Table S4.

### Supplementary Note 2.4 Qubit Overhead

The qubit overhead for each ancilla code consists of the number of data qubits for that code plus the number of ancilla qubits required to measure

Supplementary Table S3: Double-qubit gate overhead.

Gate Overhead	Gate Bound
$N_{GSC}^{(2)}$	$O((n_{MC})^3)$
$N_{RC}^{(2)}$	$O((n_{RC})^3)$
$N_{\bar{O}_{GSCH,MC}}^{(2)}$	$O((n_{MC})^4)$
$N_{\bar{H}}^{(2)}$	$O((n_{C1})^4)$
$N_{\bar{O}_{C1,C2}}^{(2)}$	$O((n_{C1})^4)$
$N_{\bar{Z}^p}^{(2)}$	$O((n_{MC})^4)$

the largest stabilizer. Only the ancillas required for largest stabilizer are included due to the presumption that a code's stabilizers will be measured sequentially. The largest of the  $GSC$  stabilizers is the modified X-stabilizer during a logical  $\bar{O}_{GSCH,MC}$  gate, which has  $2b + |\bar{O}_{MC}| = O(n_{MC})$  gates. Then, as a Shor-style measurement requires one qubit per gate, the total number of additional qubits required per  $GSC$  ancilla register is up to

$$\begin{aligned} n_{\bar{O}_{GSCH,MC}} &= O(n_{GSC} + n_{MC}) \\ &= O((n_{MC})^2). \end{aligned} \tag{S9}$$

Furthermore, each  $RC$  stabilizer cannot have more than  $n_{RC}$  gates and thus requires  $n_{\bar{Z}^p} = O(n_{RC})$  total additional qubits.

Table S5 lists the qubit overhead associated with each stabilizer-generic gate and the components contributing to it.

Supplementary Table S4: Single-qubit gate overhead.

Gate Overhead	Expression / Gate Bound
$N_{GSC}^{(1)}$	$t_{GSC}$ $O(d_{C1})$
$N_{RC}^{(1)}$	$t_{RC}$ $O(d_{C1})$
$N_{\bar{O}_{GSCH,MC}}^{(1)}$	$aN_{GSC}^{(1)}$ $\leq (d_{C1})^2$
$N_{\bar{H}}^{(1)}$	$2N_{\bar{O}_{GSCH,C1}}^{(1)}$ $O((d_{C1})^2)$
$N_{\bar{O}_{C1,C2}}^{(1)}$	$N_{\bar{O}_{GSCH,C1}}^{(1)} + N_{\bar{H}}^{(1)} + N_{\bar{O}_{GSCH,C1}}^{(1)}$ $O((d_{C1})^2)$
$N_{\bar{Z}^p}^{(1)}$	$N_{\bar{O}_{C1,RC}}^{(1)} + n_{RC} + N_{GSC}^{(1)} + N_{RC}^{(1)} + N_{\bar{O}_{C1,RC}}^{(1)}$ $O((d_{C1})^2 + n_{RC})$
$N_{\bar{T}}^{(1)}$	$O((d_{C1})^2 + n_{TC})$ $O((d_{C1})^2 \log^2 d_{C1})$

Supplementary Table S5: Qubit overhead for stabilizer-generic gates.

Gate	# of GSC	# of RC	Expression / Qubit Bound
$\bar{H}$	1	0	$n_{\bar{O}_{GSCH,C1}}$ $O((n_{C1})^2)$
$\bar{O}_{C1,C2}$	2	0	$2n_{\bar{O}_{GSCH,C1}}$ $O((n_{C1})^2)$
$\bar{Z}^p$	2	1	$2n_{\bar{O}_{GSCH,MC}} + n_{\bar{Z}^p}$ $O((n_{MC})^2)$

### Supplementary Note 3 Triorthogonal Bounds

Haah and Hastings presented efficient protocols to generate triorthogonal matrices with distance  $d_T = \Omega\left(\frac{\sqrt{n_T}}{\log n_T}\right)$  [17]. This implies that

$$d_T = \Omega\left(\frac{\sqrt{n_T}}{\log n_T}\right) \quad (\text{S10})$$

$$\frac{\sqrt{n_T}}{\log n_T} = O(d_T) \quad (\text{S11})$$

$$\sqrt{n_T} = O(d_T \log n_T) \quad (\text{S12})$$

$$n_T = O((d_T)^2 \log^2 n_T) \quad (\text{S13})$$

$$(\text{S14})$$

To get  $\log n_T$  in terms of  $d_T$ ,

$$n_T = O((d_T)^2 \log^2 n_T) \quad (\text{S15})$$

$$\log n_T = O(\log(d_T)^2) + \log(\log^2 n_T) \quad (\text{S16})$$

$$= O(2 \log d_T) + 2 \log(\log n_T) \quad (\text{S17})$$

$$= O(\log d_T) \quad (\text{S18})$$

$$(\text{S19})$$

Thus,

$$n_T = O\left((d_T)^2 \log^2 n_T\right) \quad (\text{S20})$$

$$= O\left((d_T)^2 \log^2 d_T\right) \quad (\text{S21})$$

## Supplementary Note 4 Equations and Examples

The following sections use these shorthand notations:

$$\begin{aligned} |\tilde{\psi}\rangle_{C1} &= \bar{X}_{C1} |\psi\rangle_{C1} \\ &= \alpha |1\rangle_{C1} + \beta |0\rangle_{C1} \\ |\hat{\psi}\rangle_{C1} &= \bar{Z}_{C1} |\psi\rangle_{C1} \\ &= \alpha |0\rangle_{C1} - \beta |1\rangle_{C1} \\ |\hat{\tilde{\psi}}\rangle_{C1} &= \bar{Z}_{C1} \bar{X}_{C1} |\psi\rangle_{C1} \\ &= \beta |0\rangle_{C1} - \alpha |1\rangle_{C1} \end{aligned} \quad (\text{S22})$$

### Supplementary Note 4.1 Hadamard, Fault-Intolerant

The following details the action of the first four operations of the stabilizer-generic Hadamard gate.

$$\begin{aligned} &H_A \bar{Z}_{A,C1} \bar{X}_{A,C1} H_A (|0\rangle_A |\psi\rangle) \\ &= H_H \bar{Z}_{A,C1} \bar{X}_{A,C1} (|+\rangle_A |\psi\rangle) \\ &= H_A \bar{Z}_{A,C1} (|0\rangle_A |\psi\rangle + |1\rangle_A |\tilde{\psi}\rangle) \\ &= H_A (|0\rangle_A |\psi\rangle + |1\rangle_A |\hat{\tilde{\psi}}\rangle) \\ &= |+\rangle_A |\psi\rangle + |-\rangle_A |\hat{\tilde{\psi}}\rangle \\ &= |+\rangle_A (\alpha |0\rangle_{C1} + \beta |1\rangle_{C1}) + |-\rangle_A (\beta |0\rangle_{C1} - \alpha |1\rangle_{C1}) \\ &= \alpha |0\rangle_A |0\rangle_{C1} + \beta |0\rangle_A |1\rangle_{C1} + \alpha |1\rangle_A |0\rangle_{C1} + \beta |1\rangle_A |1\rangle_{C1} \\ &\quad - \alpha |0\rangle_A |1\rangle_{C1} + \beta |0\rangle_A |0\rangle_{C1} + \alpha |1\rangle_A |1\rangle_{C1} - \beta |1\rangle_A |0\rangle_{C1} \\ &= |0\rangle_A ((\alpha + \beta) |0\rangle_{C1} + (\beta - \alpha) |1\rangle_{C1}) \\ &\quad + |1\rangle_A ((\alpha - \beta) |0\rangle_{C1} + (\alpha + \beta) |1\rangle_{C1}) \end{aligned} \quad (\text{S23})$$

### Supplementary Note 4.2 Controlled-Flips, Fault-Intolerant

The following details the action of the first four operations of the stabilizer-generic flip gate.

Supplementary Table S6: The stabilizers for the Multiple Cat Code with 3 cat states and 4 qubits per cat state ( $GSC_{3,4}$ ), having generators  $g_i$  and logical operators  $\bar{Z}$  and  $\bar{X}$ .

Name	Operator
$g_0$	$Z_0Z_1$
$g_1$	$Z_1Z_2$
$g_2$	$Z_2Z_3$
$g_3$	$Z_4Z_5$
$g_4$	$Z_5Z_6$
$g_5$	$Z_6Z_7$
$g_6$	$Z_8Z_9$
$g_7$	$Z_9Z_{10}$
$g_8$	$Z_{10}Z_{11}$
$g_9$	$X_0X_1\dots X_7$
$g_{99}$	$X_4X_5\dots X_{11}$
$\bar{Z}$	$X_0X_1X_2X_3$
$\bar{X}$	$Z_0Z_4Z_8$

$$\begin{aligned}
& H_A \bar{O}_{A,C2} H_A \bar{Z}_{A,C1} H_A (|0\rangle_A |\psi\rangle_{C1} |\phi\rangle_{C2}) \\
&= H_A \bar{O}_{A,C2} H_A \bar{Z}_{A,C1} (|+\rangle_A |\psi\rangle_{C1} |\phi\rangle_{C2}) \\
&= H_A \bar{O}_{A,C2} H_A (|0\rangle_A |\psi\rangle_{C1} + |1\rangle_A |\hat{\psi}\rangle_{C1}) |\phi\rangle_{C2} \\
&= H_A \bar{O}_{A,C2} (|+\rangle_A |\psi\rangle_{C1} + |-\rangle_A |\hat{\psi}\rangle_{C1}) |\phi\rangle_{C2} \\
&= H_A \bar{O}_{A,C2} (|0\rangle_A (|\psi\rangle_{C1} + |\hat{\psi}\rangle_{C1}) + |1\rangle_A (|\psi\rangle_{C1} - |\hat{\psi}\rangle_{C1})) |\phi\rangle_{C2} \quad (\text{S24}) \\
&= H_A \bar{O}_{A,C2} (\alpha |0\rangle_A |0\rangle_{C1} + \beta |1\rangle_A |1\rangle_{C1}) |\phi\rangle_{C2} \\
&= H_A (\alpha |0\rangle_A |0\rangle_{C1} |\phi\rangle_{C2} + \beta |1\rangle_A |1\rangle_{C1} (\bar{O}_{C2} |\phi\rangle_{C2})) \\
&= \alpha |+\rangle_A |0\rangle_{C1} |\phi\rangle_{C2} + \beta |-\rangle_A |1\rangle_{C1} (\bar{O}_{C2} |\phi\rangle_{C2}) \\
&= |0\rangle_A (\alpha |0\rangle_{C1} |\phi\rangle_{C2} + \beta |1\rangle_{C1} (\bar{O}_{C2} |\phi\rangle_{C2})) \\
&\quad + |1\rangle_A (\alpha |0\rangle_{C1} |\phi\rangle_{C2} - \beta |1\rangle_{C1} (\bar{O}_{C2} |\phi\rangle_{C2}))
\end{aligned}$$

### Supplementary Note 4.3 Helper Code Examples

Table S6 shows the stabilizers for  $GSC_{3,4}$ , while Eq. (S25) shows the logical states of the corresponding  $GSCH_{3,4}$ .

$$\begin{aligned}
|0\rangle_{GSCH_{3,4}} &= \frac{1}{2} (|0..0..0..\rangle + |0..1..1..\rangle + |1..0..1..\rangle + |1..1..0..\rangle) \\
|1\rangle_{GSCH_{3,4}} &= \frac{1}{2} (|0..0..1..\rangle + |0..1..0..\rangle + |1..0..0..\rangle + |1..1..1..\rangle)
\end{aligned} \tag{S25}$$

where  $|a..b..c..\rangle$  is shorthand for  $|a\rangle^{\otimes 4} |b\rangle^{\otimes 4} |c\rangle^{\otimes 4}$ .